Investigating controls on mineralisation in the Batten Fault Zone using numerical models

Heather A Sheldon[1,2] *and Peter M Schaubs*[1]

Introduction

The McArthur River (HYC) Pb-Zn-Ag deposit is a large stratiform sediment-hosted deposit located in the Batten Fault Zone of the southern McArthur Basin (**Figure 1**). The ca 1640 Ma deposit occurs in relatively un-deformed dolomitic siltstones of the Barney Creek Formation (McArthur Group). It is believed to have formed by reduction of an oxidised basinal brine interacting with anoxic sediments at or just below the sea floor (eg Logan *et al* 2001; Rye and Williams 1981; Eldridge *et al* 1993; Hinman 1995; Large *et al* 1998). This brine likely originated from evaporitic deposits deeper in the basin, and leached metals from deeply buried volcanic units before returning to the surface via the Emu Fault on the eastern side of the Batten Fault Zone (Williford *et al* 2011; Cooke *et al* 1998; Large *et al* 1998). However, questions remain as to the fluid flow drivers and pathways that controlled this mineral system and its location within the Batten Fault Zone. This study aims to address these questions by using numerical models to explore patterns of fluid flow in simple fault architectures representing aspects of the Batten Fault Zone at the time of mineralisation. We simulate fluid flow driven by density (ie convection) and deformation under varying stress regimes in order to identify key controls on the fluid flow regime within the known architecture.

Geological setting

The McArthur Basin comprises a Palaeo- to Mesoproterozoic succession of carbonate and siliciclastic units with minor volcanic units, deposited in an intracratonic setting (Rawlings *et al* 2004; Betts *et al* 2003). The basin-fill is divided into 4 groups. The Tawallah Group is dominated by shallow marine to fluvial sandstones, with minor mudstone, dolostone and volcanic intervals. Volcanic units of the upper Tawallah Group have been interpreted as the source of metals for the HYC deposit (Cooke *et al* 1998) with permeable sandstones and faults providing a pathway for the metal-charged fluid to reach the seafloor (Large *et al* 1998; Garven *et al* 2001). The Tawallah Group is overlain by the McArthur Group, which comprises interbedded dolostones, sandstones, mudstones and minor tuffaceous mudstones, deposited primarily in shallow water environments. The McArthur Group includes the Barney Creek Formation, which hosts the HYC deposit. The remaining two groups, the Nathan and Roper groups, postdate mineralisation at HYC and are not relevant to this study.

Previous numerical modelling studies

Previous numerical modelling studies of the HYC mineralising system focused on fluid flow driven by topography and density, with the density variations related to temperature and/or salinity of the pore fluid (eg Garven *et al* 2001; Yang *et al* 2004a; Yang *et al* 2004b; Yang 2006). The first studies were based on a simple 2D cross-section of the Batten Fault Zone (**Figure 2**), comprising

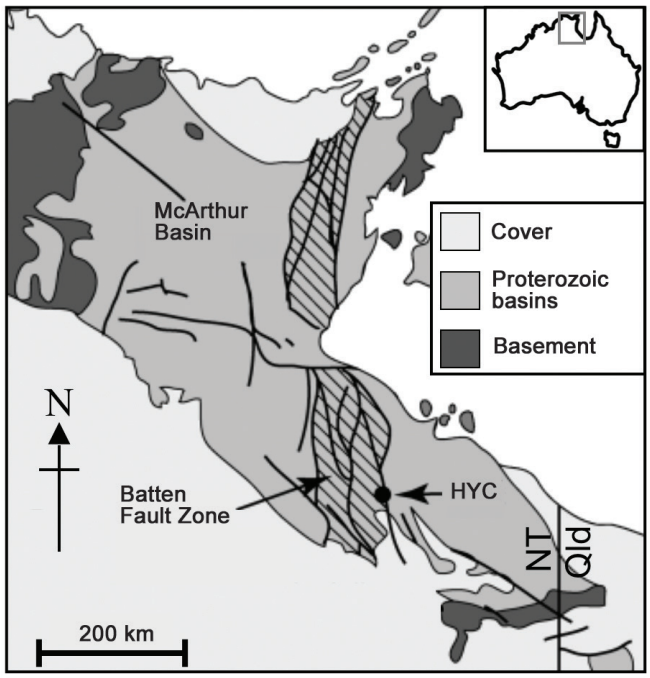

Figure 1. Location of the Batten Fault Zone and HYC deposit within the McArthur Basin, Northern Territory, Australia. Modified from Garven *et al* (2001).

[1] CSIRO Mineral Resources, 26 Dick Perry Avenue, Kensington WA 6151, Australia
[2] Email: heather.sheldon@csiro.au

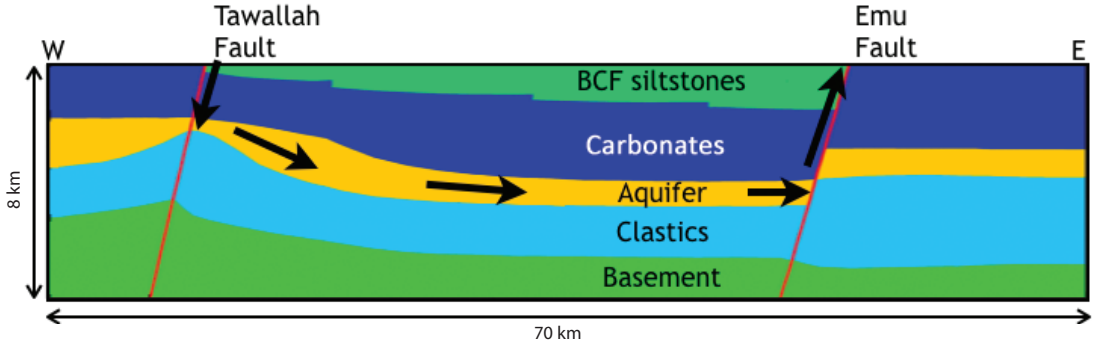

Figure 2. Simple 2D geometry used in previous numerical modelling studies (modified from Yang *et al* 2004a). Vertical exaggeration x2. Stratigraphy: BCF siltstones and Carbonates = McArthur Group. Aquifer = lower McArthur Group and Upper Tawallah Group. Clastics = Tawallah Group. Aquifer and faults have high permeability; other units have low permeability (see **Table 1**). Arrows indicate general pattern of fluid flow predicted by numerical models.

two west-dipping faults (the Tawallah and Emu faults, representing the boundaries of the Batten Fault Zone) intersecting a simplified stratigraphic sequence. The results of these studies suggested that fluid would flow down the Tawallah Fault, then through an aquifer unit representing siliciclastics and volcanics of the upper Tawallah Group where it would scavenge metals, and then flow up the Emu Fault to the seafloor where mineralisation could take place.

Yang (2006) expanded the model into 3 dimensions by extrapolating the 2D model along strike of the faults, and found that the dominant convective flow pattern switched to one of convection within the plane of the faults with very little fluid passing through the aquifer unit between the faults. The only way to achieve significant fluid flow between the faults (as in previous 2D studies) was to introduce a cross-fault connecting the Tawallah and Emu faults.

While these studies have provided useful insights into some aspects of the fluid flow regime in the Batten Fault Zone, they did not consider the effect of deformation on fluid flow. Deformation influences fluid flow by driving fluid away from areas of contraction and towards areas of dilation. Depending on the strain rate, deformation may override density and topography to become the dominant fluid flow driver. In particular, fluid tends to move downwards during extensional deformation, making it more difficult to achieve the strong upward flow that is required to explain the return of the metal-charged brine from depth to the seafloor. This is particularly relevant to mineralisation at HYC as the geological evidence indicates that the Barney Creek Formation was deposited in a rapidly subsiding sub-basin adjacent to the Emu Fault, implying relatively high strain rates in an extensional or strike-slip tectonic setting (e.g. Rawlings *et al* 2004; Betts *et al* 2003). Hence, we build on the previous modelling studies by including deformation, and investigate the competition between deformation and density as fluid flow drivers.

Modelling approach

To explore the competition between different fluid flow drivers we use the open-source finite element solver MOOSE (Multiphysics Object Oriented Simulation Environment) to solve the coupled partial differential equations that describe conservation of mass, momentum and energy in a deforming porous medium. The rock is treated as an elastic-plastic porous medium in which the pore space is completely saturated with a single pore fluid (water). Plasticity is represented by the Drucker-Prager constitutive law with a tensile cut-off; fluid flow is assumed to obey Darcy's law. Heat is transported by conduction and advection with the moving pore fluid. The pore fluid moves in response to changes in fluid pressure caused by deformation and to changes in density associated with the temperature gradient. Details of the equations and solution technique can be found in the MOOSE documentation (CSIRO and INL 2018). **Table 1** lists the rock properties used in the simulations.

In this contribution, we present results obtained using two simple geometries representing aspects of the Batten Fault Zone. The first geometry represents a steeply dipping, north-south striking normal fault intersecting a horizontally layered sequence (**Figure 3a**) using the same layering as in previous modelling studies (**Figure 2**). With this simple

Table 1. Rock properties used in the models.

Property	BCF	Carbonate	Aquifer	Clastics	Basement	Faults
Cohesion (MPa)	20	22	20	27	24	1
Tensile strength (MPa)	2	2.2	2	2.7	2.4	0.1
Friction angle (°)	20	30	25	28	30	15
Bulk modulus (GPa)	6	30	20	27	30	10
Shear modulus (GPa)	6	20	5	7	25	2
Horizontal permeability (10^{-15} m^2)	1	10	100	1	0.01	100
Vertical permeability (10^{-15} m^2)	0.01	0.1	1	0.01	0.01	100
Porosity (-)	0.3	0.1	0.15	0.05	0.01	0.05
Thermal conductivity (W/m/K)	2.9	2.8	3.5	3.5	3	3.2
Specific heat capacity (J/kg/K)	850	850	850	850	850	850

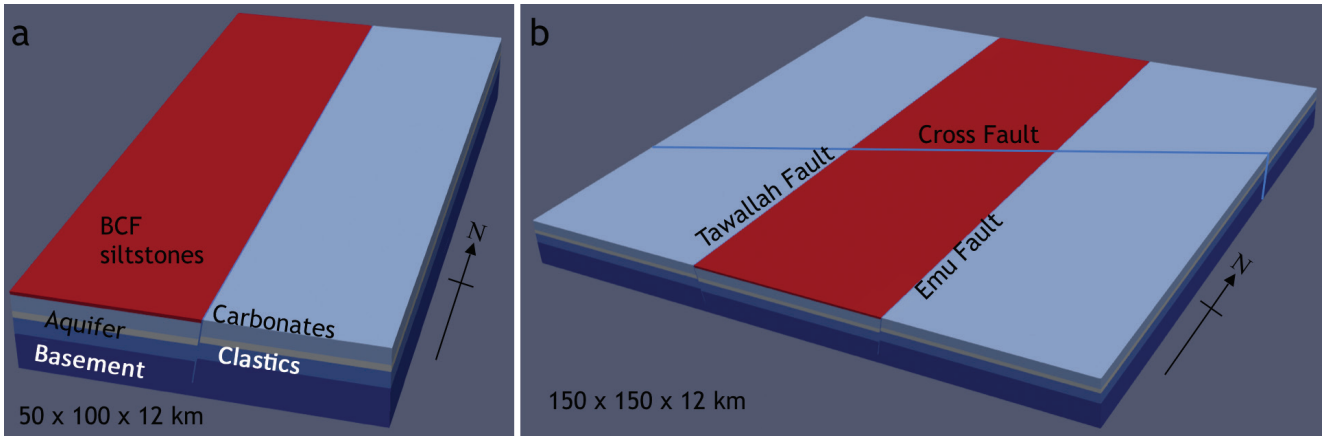

Figure 3. Geometry of numerical models in this study. (**a**) Model with single fault. (**b**) Model with Tawallah and Emu faults and a cross fault. BCF = Barney Creek Formation.

geometry, we investigate the interplay between east–west extensional deformation and thermal convection in the fault.

The second geometry represents the Tawallah and Emu faults, intersected by a cross-fault striking east-northeast–west-southwest (**Figure 3b**). In this model, we impose sinistral strike-slip deformation on the north-south model boundaries, and again observe the interplay between deformation and thermal convection.

In both models, the top boundary represents the seafloor with fluid pressure corresponding to a water depth of 200 m and temperature 20°C, consistent with the inferred depositional environment of the Barney Creek Formation (Schmid 2015). The top boundary temperature is fixed except in the faults, where the temperature is that of the pore fluid where fluid is flowing out of the model, and is 20°C where fluid is flowing into the model. The initial fluid pressure gradient is hydrostatic. The base of the model is subject to a fixed heat flux of 70 mW/m^2, corresponding to a geothermal gradient of ~20–30°C/km depending on the thermal conductivity, which varies between the stratigraphic units (**Table 1**).

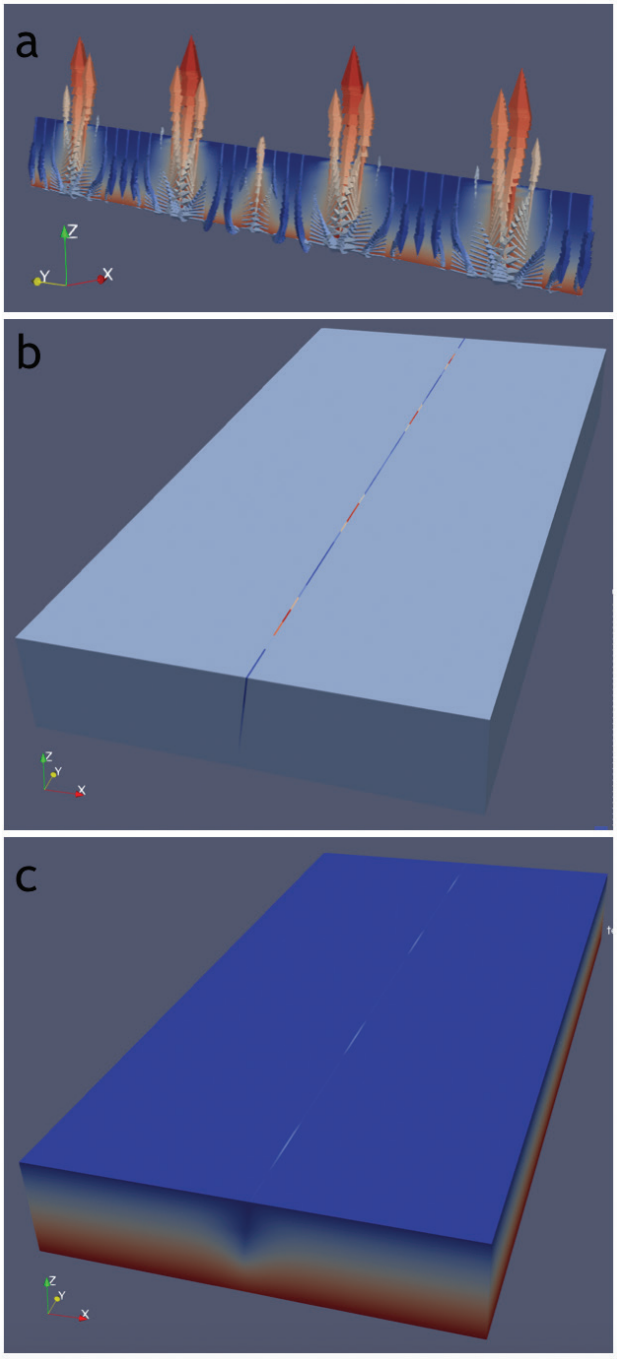

Figure 4. Temperature and fluid flux in the single fault model at low strain rate. (**a**) Temperature contours (20–270°C) and fluid flow vectors in the fault. Vectors scaled by flux magnitude and coloured by vertical component of fluid flux (-2 x 10^{-8} – 4 x 10^{-8} m/s). (**b**) Vertical component of fluid flux (-2 x 10^{-8} – 4 x 10^{-8} m/s), whole model. (**c**) Temperature (20–313 °C), whole model.

Results

Figure 4 illustrates the fluid flow patterns and temperature distribution in the first model when it is subject to a slow extensional strain rate of 10^{-17} s^{-1}. The dominant flow pattern is one of thermal convection in the plane of the fault, with temperatures reaching 100°C at the seafloor. Once convection has been established, the strain rate is increased to a higher value in order to observe the effect of deformation-driven flow on convection. **Figure 5** shows the evolution of the maximum and minimum vertical fluid flux in the fault; this is a measure of strength of the convective flow. Negative values imply downward flow, positive values imply upward flow. The strain rate is increased from 10^{-17} s^{-1} to a higher value (10^{-16} s^{-1}, 10^{-15} s^{-1}, 10^{-14} s^{-1} or 10^{-13} s^{-1}) after 2 x 10^{13} s (0.63 million years; this

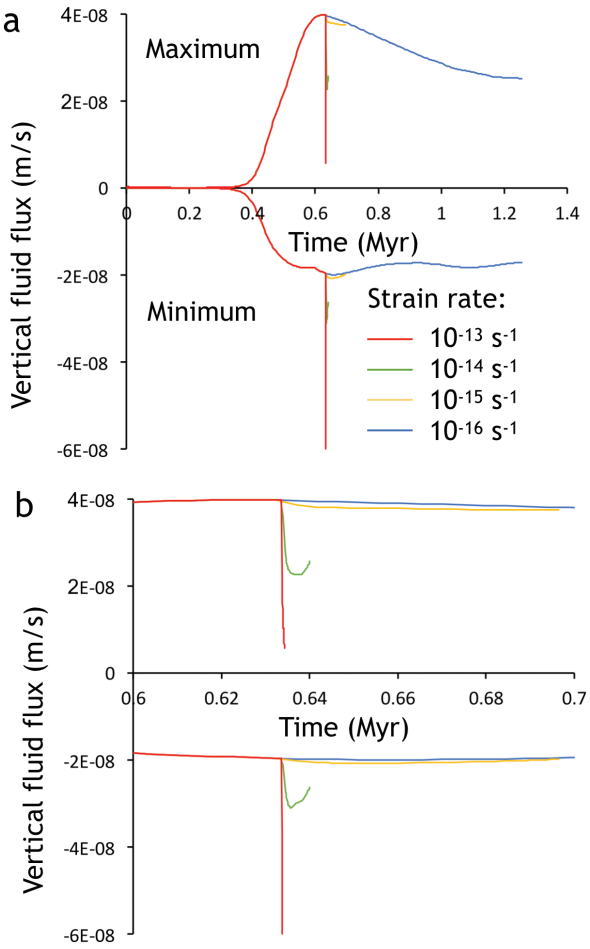

Figure 5. Evolution of the maximum and minimum vertical fluid flux in the single fault model. Strain rate is increased from 10^{-17} s^{-1} to a higher value (indicated in legend) after 2 x 10^{13} s (0.63 million years). (**a**) Duration of model. (**b**) Detail of behaviour immediately before and after increase in strain rate.

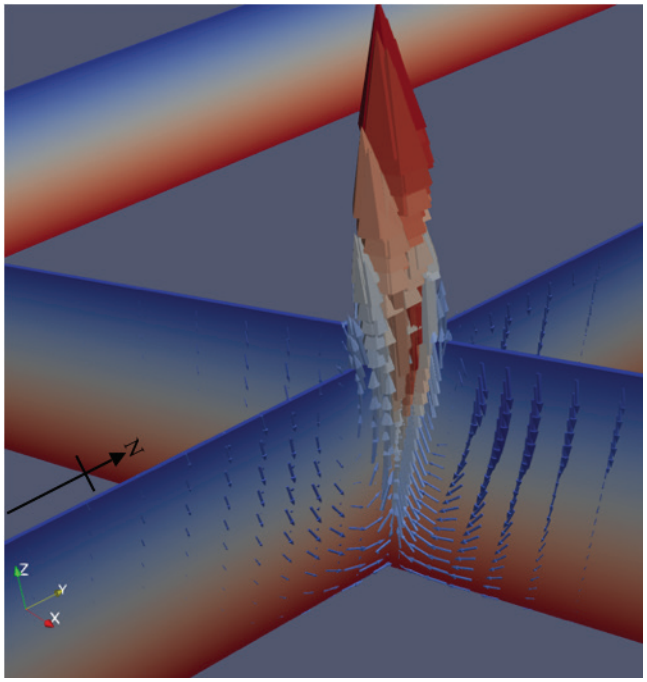

Figure 6. Convection around fault intersection in the model with a cross fault. Temperature contours (20–270°C) and fluid flow vectors in the fault. Vectors scaled by flux magnitude and coloured by vertical component of fluid flux (-0.2 x 10^{-8}–1.4 x 10^{-8} m/s).

time was chosen for being sufficient to allow convection to be established in the faults, but it does not have any geological significance). At the highest strain rate, the maximum and minimum fluid flux are dramatically reduced; whereas at the lower strain rates, the fluid flux at first decreases but then begins to recover. These patterns reflect the tendency for extensional deformation to drive downward flow.

Computational limitations prevented running the simulations long enough to determine whether the convective fluid flux would eventually recover at the higher strain rates. However, the results do show that convective flow would at least be disrupted at moderate to high strain rates. It is possible that convective flow may be overridden completely at strain rates higher than those investigated here.

Figure 6 illustrates the behaviour of the second geometry when subject to sinistral strike-slip deformation imposed on the north-south boundaries of the model at a strain rate of 10^{-15} s^{-1}. In this case, the results show localised convective upwelling at the fault intersections with downwelling immediately adjacent to these points.

Discussion and future directions

Formation of the HYC deposit involved fluid ascending from depth, probably along the Emu Fault or related structures. The simulation results presented here, and those of previous modelling studies, suggest that convection may have contributed to this upward flow. However, we have also shown that deformation at moderate strain rates can disrupt convective flow; at higher strain rates the convective flow might be overridden completely by downward, deformation-driven flow. Thus, if convection played a role in this system, it seems likely that it would have been during a hiatus in deformation. The presence of alternating fine-grained sediments and breccias in the Barney Creek Formation (Large *et al* 1998) is suggestive of intermittent high strain rate events, interspersed with periods of lower strain rate when convection may have been established. Our results also suggest that fault intersections may have been important conduits for upward flow, consistent with the occurrence of deposits close to fault intersections in the Batten Fault Zone (Betts *et al* 2003).

In the models presented here, fluid flow is predominantly within the faults, with little interaction between the fluid and the likely source rocks of the metals (ie the aquifer). Thus these models alone cannot explain formation of the HYC deposit as this mineralisation required interaction of a large volume of fluid with the source rocks. The same problem was encountered in an earlier 3D modelling study, which also found fluid flow being largely restricted to the faults (Yang 2006). Further investigation is required to identify conditions under which sufficient volumes of fluid would have moved through the source rocks to account for the observed mineralisation. Critical factors in achieving such flow patterns may include salinity gradients, spatial and temporal variations in permeability in the faults and host rocks, and geometric complexities such as variations in dip and thickness of the rock units. Future modelling work will explore these factors with the aim of better understanding the mineralising system at HYC.

Acknowledgements

Simulations were run on supercomputing facilities provided by the Pawsey Supercomputing Centre and CSIRO. Andy Wilkins (CSIRO) is acknowledged for his support in developing the necessary modules for MOOSE.

References

Betts PG, Giles D and Lister GS, 2003. Tectonic environment of shale-hosted massive sulfide Pb-Zn-Ag deposits of Proterozoic Northeastern Australia. *Economic Geology* 98, 557–576.

Cooke DR, Bull SW, Donovan S and Rogers JR, 1998. K-metasomatism and base metal depletion in volcanic rocks from the McArthur Basin Northern Territory; Implications for base metal mineralization. *Economic Geology* 93, 1237–1263.

CSIRO and INL, 2018. *MOOSE's PorousFlow Module*. https://github.com/idaholab/moose/raw/devel/modules/porous_flow/doc/theory/theory.pdf.

Eldridge CS, Williams N and Walshe JL, 1993. Sulfur isotope variability in sediment-hosted massive sulfide deposits as determined using the ion microprobe SHRIMP; II, A study of the HYC deposit at McArthur River, Northern Territory, Australia. *Economic Geology* 88, 1–26.

Garven G, Bull SW and Large RR, 2001. Hydrothermal fluid flow models of stratiform ore genesis in the McArthur Basin, Northern Territory, Australia. *Geofluids* 1, 289–311.

Hinman MC, 1995. Base metal mineralization at McArthur River: Structure and kinematics of the HYC-Cooley zone at McArthur River. *Australian Geological Survey Organisation Record* 1995/5.

Large RR, Bull SW, Cooke DR and McGoldrick PJ, 1998. A genetic model for the HYC deposit, Australia; Based on regional sedimentology geochemistry and sulfide-sediment relationships. *Economic Geology* 93, 1345–1368.

Logan GA, Hinman MC, Walter MR and Summons RE, 2001. Biogeochemistry of the 1640 Ma McArthur River (HYC) lead-zinc ore and host sediments, Northern Territory, Australia. *Geochimica et Cosmochimica Acta* 65, 2317–2336.

Rawlings DJ, Korsch RJ, Goleby BR, Gibson GM, Johnstone DW and Barlow M, 2004. The 2002 Southern McArthur Basin seismic reflection survey. *Geoscience Australia Record* 2004/17.

Rye DM and Williams N, 1981. Studies of the base metal sulfide deposits at McArthur River, Northern Territory, Australia: III, the stable isotope geochemistry of the HYC, Ridge and Cooley deposits. *Economic Geology* 76, 1–26.

Schmid S, 2015. Sedimentological review of the Barney Creek Formation in drillholes LV09001, BJ2, McA5, McArthur Basin. *Northern Territory Geological Survey Record* 2015-006.

Williford KH, Grice K, Logan GA, Chen J and Huston D, 2011. The molecular and isotopic effects of hydrothermal alteration of organic matter in the Paleoproterozoic McArthur River Pb/Zn/Ag ore deposit. *Earth And Planetary Science Letters* 301, 382–392.

Yang J, Bull SW and Large RR, 2004a. Numerical investigation of salinity in controlling ore-forming fluid transport in sedimentary basins: Example of the HYC deposit, Northern Australia. *Mineralium Deposita* 39, 622–631.

Yang J, Large RR and Bull SW, 2004b. Factors controlling free thermal convection in faults in sedimentary basins: Implications for the formation of zinc-lead mineral deposits. *Geofluids* 4, 237–247.

Yang J, 2006. Full 3-D Numerical Simulation of hydrothermal fluid flow in faulted sedimentary basins: Example of the Mcarthur Basin, Northern Australia. *Journal of Geochemical Exploration* 89, 440–444.